MODELING OXYGEN AND CARBON DIOXIDE TRANSPORT AND EXCHANGE USING A CLOSED LOOP CIRCULATORY SYSTEM

Brian E. Carlson, Joseph C. Anderson, Gary M. Raymond, Ranjan K. Dash, and James B. Bassingthwaighte [*]

Abstract: The binding and buffering of O_2 and CO_2 in the blood influence their exchange in lung and tissues and their transport through the circulation. To investigate the binding and buffering effects, a model of blood-tissue gas exchange is used. The model accounts for hemoglobin saturation, the simultaneous binding of O_2, CO_2, H^+, 2,3-DPG to hemoglobin, and temperature effects.[1,2] Invertible Hill-type saturation equations facilitate rapid calculation of respiratory gas redistribution among the plasma, red blood cell and tissue that occur along the concentration gradients in the lung and in the capillary-tissue exchange regions. These equations are well-suited to analysis of transients in tissue metabolism and partial pressures of inhaled gas. The modeling illustrates that because red blood cell velocities in the flowing blood are higher than plasma velocities after a transient there can be prolonged differences between RBC and plasma oxygen partial pressures. The blood-tissue gas exchange model has been incorporated into a higher level model of the circulatory system plus pulmonary mechanics and gas exchange using the RBC and plasma equations to account for pH and CO_2 buffering in the blood.

1. INTRODUCTION

The exchange of O_2 and CO_2 between the tissue and vasculature depends on adequate delivery and removal of these gases. Oxygen delivery begins with inhalation of ambient air into the airspaces of the lung, transport to the blood from the alveoli, transport through the arterial system, and then exchange between the blood and the peripheral tissue. In a closed circulatory system, venous blood returns to the lungs where

[*] Brian E. Carlson, Joseph C. Anderson, Gary M. Raymond, and James B. Bassingthwaighte, Department of Bioengineering, University of Washington, Seattle, Washington, 98195. Ranjan K. Dash, Department of Physiology, Medical College of Wisconsin, Milwaukee, Wisconsin, 53226.

CO_2 is expired. Quantifying O_2 and CO_2 transport requires accounting for their solubility in plasma, RBCs and tissue as well as their binding and release from the hemoglobin (Hb) in the RBCs and, in addition, for O_2 only, its binding to myoglobin in tissue. Hemoglobin dissociation curves were developed that described the fraction of O_2 and CO_2 bound to Hb in the steady state as a function of P_{O2}, P_{CO2}, pH, 2,3-DPG and temperature.[1] These expressions were used to describe the steady state transport of O_2 and CO_2 as well as H^+ and HCO_3^- in a blood-tissue exchange model with convective transport and axial diffusion in the capillary along with exchange and metabolism in the surrounding tissue region.[2]

The model presented in this study accounts for ventilatory exchange between outside air and lung alveoli, exchange with alveolar capillary blood, convective transport in arteries, the exchange in tissue capillaries and arterioles, and return of venous blood to the lungs. The model describes transport of O_2 and CO_2 to tissue as influenced by respiration rate, composition of inspired gas, H^+ and CO_2 production and O_2 consumption in tissue and buffering in the blood.

A feature of biophysical interest but modest physiological importance is the persistence of disequilibria between plasma and RBC P_{O2} due to the higher velocities of RBC than plasma. This difference in velocity exists in all regions of the vasculature but is at a maximum in the microcirculation. Bloch[3] observed the existence of a layer of plasma close to the vessel wall, which he called the peripheral plasma layer. The average ratio of total layer thickness to vessel inside diameter was 1:4 in the 5-10 μm capillariies in Bloch's study, which agrees with more recent observations of the endothelial surface layer seen by Vink and Duling.[4] Because this layer is close to the capillary wall the velocity of the plasma in that region is slower than the centerline axial velocity of the RBCs. To quantify the relative velocity ratio of RBC to plasma we have looked at indicator dilution studies that document the mean transit time of RBC-tagged versus plasma-tagged indicators by Goresky.[5] Goresky showed that the mean transit time of RBCs was on the order of 2/3 of that of the plasma through the entire hepatic vasculature.

2. DESCRIPTION OF THE MODEL

2.1. Lung-Blood Exchange Region

The lung module is composed of three serial compartments[6]: a low compliance compartment representing the oral/nasal cavity and the cartilaginous airways, a moderately compliant compartment characterizing the collapsible bronchial airways and a high compliance compartment resembling the alveolar space. In the model, the lung can be ventilated by positive pressure or by periodic chest expansion reducing intrapleural pressure, both resulting in bi-directional airflow and inflation and deflation of the lung. Convective flow between compartments is modeled as pressure-driven flow through a resistance. Equations for convective and diffusive transport of oxygen and carbon dioxide between adjacent lung compartments are similar to those used in previous models.[6] Each lung compartment is assumed to be well-mixed. The alveolar compartment exchanges respiratory gases with the plasma region of a blood-tissue exchange unit,[2] which contains a region of red cells surrounded by a plasma region. The inhaled partial pressure of each species is a model input.

2.2. Blood-Tissue Exchange Region

Figure 1 shows a previously described one-dimensional blood-tissue exchange model.[2] The lumen of a permeable vessel is divided into a flowing core of RBCs surrounded by a plasma sleeve. Hemoglobin binding is represented in the RBC region by the invertible hemoglobin dissociation expressions.[1] The exchange vessel endothelial barrier is treated as purely passive and is surrounded by an interstitial fluid layer giving access to parenchymal cells. In the parenchymal cells, where myoglobin buffers O_2, oxygen is consumed and CO_2 is produced in accord with the respiratory quotient: RQ = moles CO_2 per mole O_2 and a specified metabolic rate. Each region is axially-distributed, exhibiting concentration gradients from entrance to exit but well-mixed radially, and is represented by a 1-dimensional partial differential equation. Interregional conductances, defined by the permeability surface area product (PS_x), can be adjusted to accommodate slow diffusional processes. Axial diffusion or dispersion (D_x) smoothes the axial concentration gradients.

The ratio of RBC to plasma velocity in the blood tissue exchange region was calculated using experimental morphometric data on intramyocardial arterioles and venules from Kassab et al.[7] and the reduction in hematocrit as a function of vessel diameter documented by Lipowsky.[8] In our model we have represented the blood tissue exchange region as the arterioles and capillaries smaller than 100 μm in diameter because studies by Duling and Berne[9] show significant oxygen loss in the precapillary arterioles. For porcine coronary branching trees of Kassab, flow through the blood tissue exchange region has a relative velocity ratio, v_{RBC}/v_{pl}, of 1.2 to 1.9. Therefore an intermediate value of v_{RBC}/v_{pl}, was taken as 1.5 in lung and tissue exchange regions.
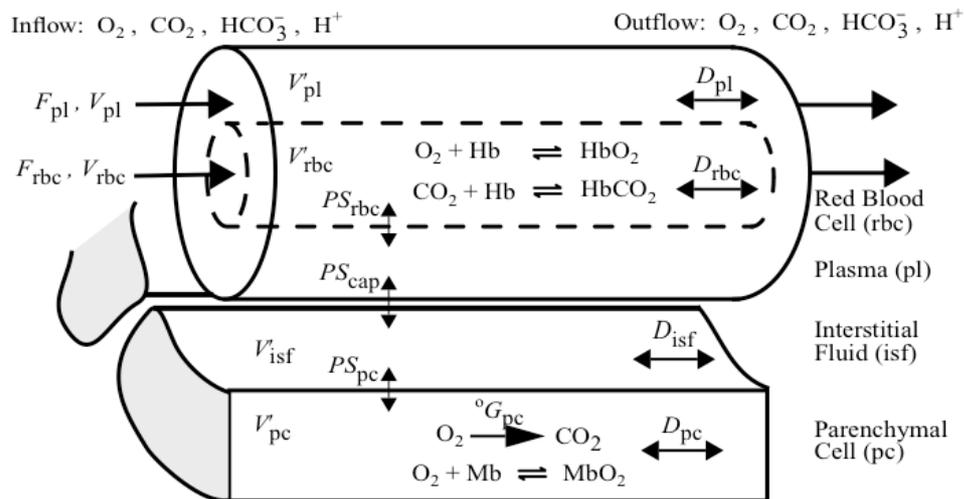

Figure 1. Blood-tissue exchange unit showing red blood cell, plasma, interstitial fluid, and parenchymal cell regions, convection of RBC and plasma, solute transport between regions, the PSs, axial diffusion, binding, and buffering within regions. Bicarbonate buffering occurs in all regions. Each region is axially-distributed and radially well-mixed.

2.3. Arterial and Venous Convective Regions

Lung capillary blood is carried through nonexchanging convective conduits (left atrium, left ventricle, aorta, arteries) to the tissue. RBC-plasma solute exchange continues. Red cell-plasma concentration differences persist when their velocities differ. Metabolism is zero, but buffering reactions continue. Values of the ratio of RBC to plasma velocity in the arteries and veins were taken to be 1.1 and 1.05 respectively, though the choice of these numbers is dependent on the range of diameters represented.

2.4 Numerical Methods and Simulation Procedures

Numerical methods are those described previously[10] using a Lagrangian sliding fluid element algorithm. Other partial differential equation solvers (MacCormack, TOMS 731) are also available under the JSim simulation system. Parameter values in this model were those used previously[2] with a few exceptions. The flow rate is allowed to range from 5 L/min at rest to 25 L/min during exercise. Also the permeability surface area product for the RBCs (PS_{RBC}) has been recalculated according to experimental evidence[11] to reflect the combination of a small hindrance to permeation of its membrane and the times required for binding and unbinding. The hemoglobin equations incorrectly assume instantaneous equilibration instead of taking several milliseconds. The lung model described here is similar in structure to the model by Lutchen et al.[6]

3. RESULTS AND DISCUSSION

Two cases are examined in this study. The first concerns respiratory gas transport during normal and elevated ventilation, perfusion, and metabolism. For normal levels, the parameters are respiratory rate of 12 breaths/min, tidal volume of ~500 ml driven by 10 mmHg of inspiratory positive pressure at the mouth for 2 seconds and inspired air with P_{O2} = 150 and P_{CO2} = 0 mmHg. Blood flow was set to ~5 L/min and metabolic rate was adjusted so pulmonary end-capillary blood partial pressures of O_2 and CO_2 were ~100 and ~40 mmHg while venous values were 70 and 45 mmHg. The end tidal P_{O2} was 105 and P_{CO2} was 34 mmHg. The second case focuses on the equilibration of O_2 between plasma and RBCs upon entering the arterial region and the effect of the relative velocity difference between plasma and RBCs on equilibration. To investigate the equilibration, the plasma partial pressure of oxygen is increased from 25 to 100 mmHg and the transient effects are observed. To investigate the effect of the relative velocity difference, a pulsed increase in plasma P_{O2} is applied at the upstream end and the difference between the plasma and RBC P_{O2} is quantified along the length of the arterial region.

3.1 Respiratory Gas Transport

Figure 2 shows that the breathing cycle causes a cyclical variation in the partial pressures of O_2 and CO_2 in bronchiolar and alveolar air and in capillary plasma. Dispersion along the airways dampens the magnitude of the fluctuations. The partial
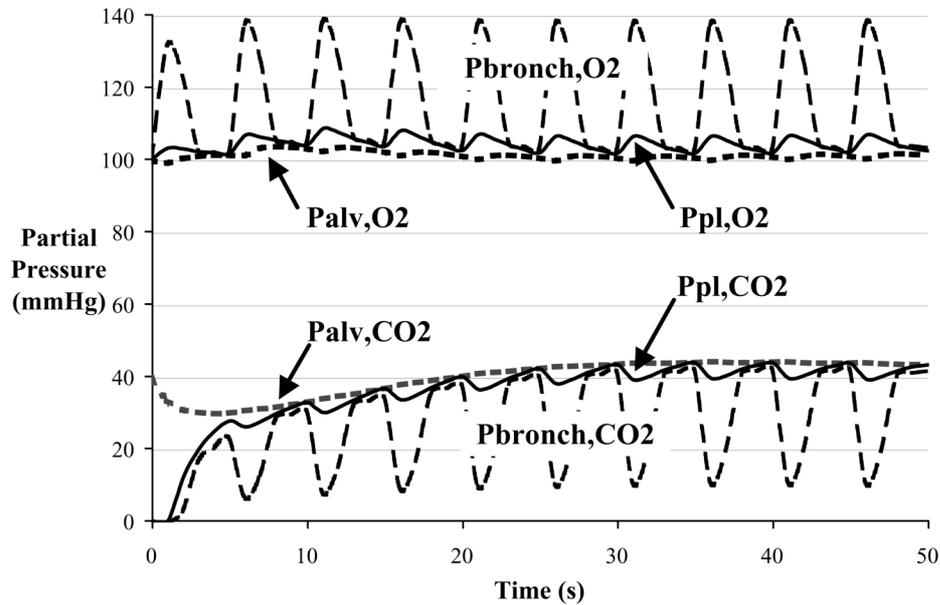
Figure 2. Displays the partial pressures of O_2 and CO_2 in the plasma region of the blood (pl), the alveoli (alv), and the collapsible airways (bronch).

pressure of CO_2 in plasma is almost unaffected by the ventilatory cycle because it is buffered by the large bicarbonate pool in the blood.

To load the red blood cell (RBC) with oxygen, oxygen moves from the well-mixed alveolar space through the plasma and into the RBC as the red blood cell moves along the length of the capillary. The relative speeds of these processes cause an axial and radial oxygen gradient to be established in the pulmonary capillary**.** Under normal conditions (given above), a large gradient between the plasma and RBC appears as the blood enters the capillary and disappears after the plasma and RBC have traveled ~40% of the capillary length (Figure 3). However, if the normal ventilation ($F_{alv,0}$) and perfusion (F_0) rate are both increased 3-fold (to offset a corresponding increase in tissue O_2 metabolism), the initial gradient between plasma and RBC increases and the two regions only equilibrate after traversing ~80% of the capillary length. A 5-fold increase in ventilation and perfusion causes the two blood components to never equilibrate while in the pulmonary capillary**.**

3.2 Disequilibrium Between pO_2 in Plasma and RBCs in Arteries

When RBC and plasma velocities are equal then equilibration across the RBC membrane occurs rapidly with a time constant governed by PS_{RBC}/V_{pl}. In contrast, when $v_{RBC}/v_{pl} > 1$ there is a continuing disequilibrium. To show this, the arterial module is isolated from the rest of the closed loop model and beginning with equilibrated P_{O2} at 25mmHg the plasma P_{O2} is increased to 100 mmHg while leaving the RBC P_{O2} unchanged. The relative velocity is given a value of 1.5 to illustrate the relative
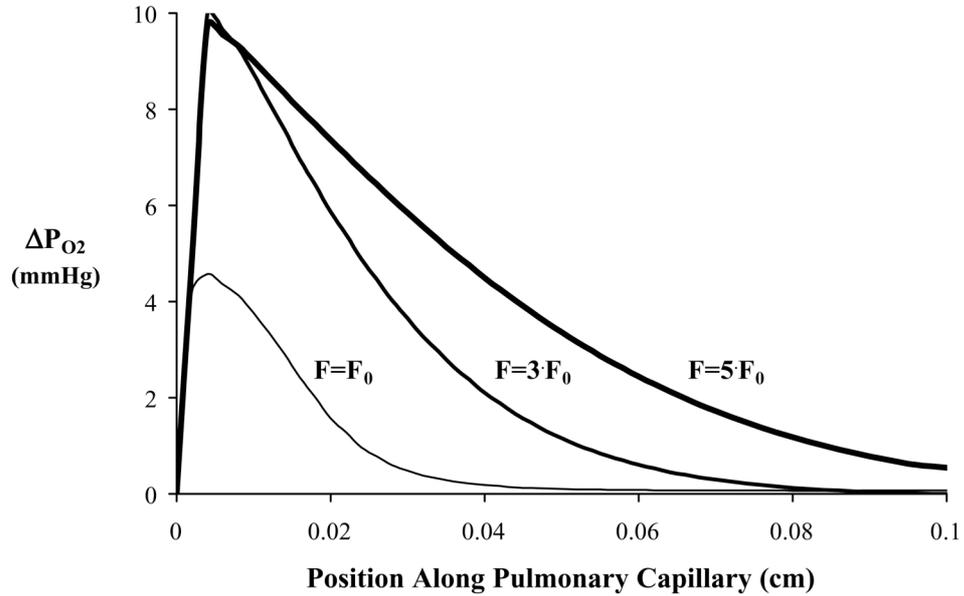
Figure 3. Oxygen partial pressure gradients between the plasma and red blood cell (ΔP_{O2}) at end-exhalation for a normal ventilation rate ($F_{alv,0}$) and blood flow (F_0) and when ventilation, blood flow, and metabolism are increased by 3-times and 5-times the normal rates. $\Delta P_{O2} = P_{O2}$ (plasma) - P_{O2} (RBC).

disequilibrium. In this simulation the concentration front has traveled about 7 cm. before the RBC and plasma concentrations equilibrate. Beyond this, the RBCs near the wavefront of heightened plasma P_{O2}, having taken up O_2, advance in the central stream ahead of the plasma front and release O_2 into the plasma where the P_{O2} is still 25 mmHg. This process of RBCs taking up O_2 behind the plasma front and then releasing it to raise the plasma P_{O2} continues. In Figure 4 are shown plots of the ΔP_{O2} across the RBC membrane as a function of position along the aorta at 4 times, a tenth of a second apart after the step increase in plasma P_{O2} at x = 0 and t = 0. Initially the ΔP_{O2} is ~75 mmHg, but is quickly dissipated as plasma O_2 enters the huge sink of the RBC Hb. Then as the RBCs that have taken up oxygen from the plasma advance ahead of the depleted plasma layer, they have a slightly higher P_{O2} than that in the plasma that had entered the tube before the pulsed increase and therefore lose oxygen to the plasma. The peak in ΔP_{O2} travels at v_{RBC} = 25 cm/s. This peak ΔP_{O2} is very small because the carrying capacity for O_2 in plasma is so small compared to that of RBC. The ΔP_{O2} is larger when RBCs are fully loaded as they travel through a region where oxygen is consumed in tissue; it is high when PS_{cap} is high compared to PS_{RBC} and low in the reverse situation. It is relevant to the interpretation of plasma P_{O2} as measured by oxygen-dependent phosphorescent probes[12].
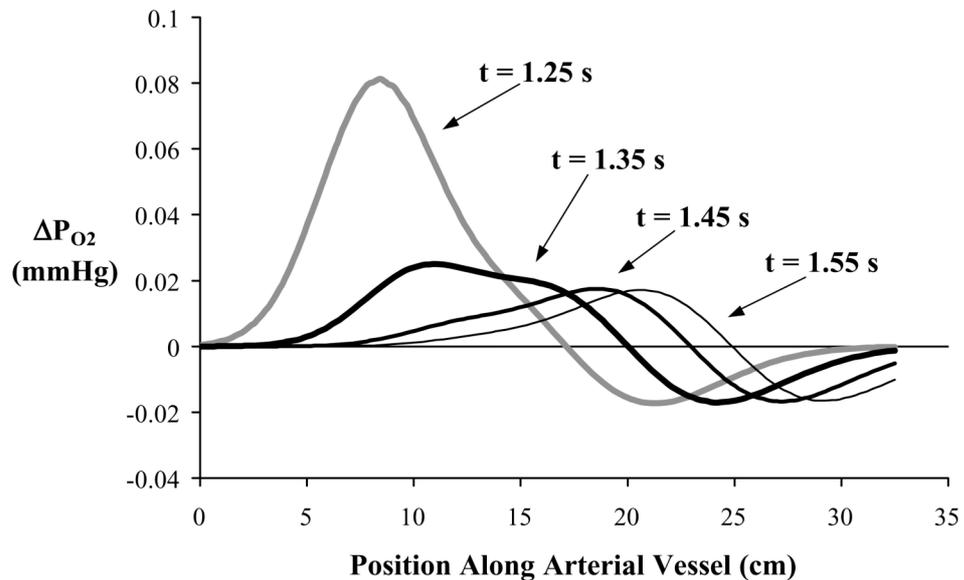
Figure 4. Difference in partial pressure of O_2 between RBC and plasma along vessel length for a Gaussian shaped pulsed increase in plasma P_{O2} at the vessel entry. The four curves represent the pulse at four different times.

4. CONCLUSIONS

We have linked together a series of blood-tissue gas exchange models with a model of gas transport in the lung to describe respiratory gas exchange between the lung and tissue via circulating blood. We illustrated that changes in metabolism causing increases in CO_2 production and O_2 consumption can be compensated by simultaneous increases in ventilation and perfusion. O_2 gradients between the plasma and red blood cell can persist along the length of the pulmonary capillary and in the arterial system because RBCs have higher velocities than plasma. The model is ideally suited for investigating questions concerning the integrative effects of pulmonary ventilation, chemical binding kinetics, vascular transport, and tissue metabolism on whole body respiratory gas exchange.

5. ACKNOWLEDGEMENT

6. REFERENCES

1. R. K. Dash and J. B. Bassingthwaighte, Blood HbO(2) and HbCO(2) dissociation curves at varied O-2, CO2, pH, 2,3-DPG and temperature levels, Ann Biomed Eng 32(12), 1676-1693 (2004).
2. R. K. Dash and J. B. Bassingthwaighte, Simultaneous blood-tissue exchange of oxygen, carbon dioxide, bicarbonate, and hydrogen ion, Ann Biomed Eng 34(7), 1129-1148 (2006).
3. E. H. Bloch, A quantitative study of the hemodynamics in the living microvascular system, Am J Anat 110(2), 125-153 (1962).
4. H. Vink and B. R. Duling, Identification of distinct luminal domains for macromolecules, erythrocytes, and leukocytes within mammalian capillaries, Circ Res 79(3), 581-589 (1996).
5. C. A. Goresky, A linear method for determining liver sinusiodal and extravascular volumes, Am J Physiol 204(4), 626-640 (1963).
6. K. R. Lutchen, F. P. Primiano and G. M. Saidel, A non-linear model combining pulmonary mechanics and gas concentration dynamics, IEEEE Trans Biomed Eng 29(9), 629-641 (1982).
7. G. S. Kassab, C. A. Rider, N. J. Tang and Y. C. B. Fung, Morphometry of pig coronary arterial trees, Am J Physiol Heart Circ Physiol 265(1), H350-H365 (1993).
8. H. H. Lipowsky, S. Usami and S. Chien, Invivo measurements of apparent viscosity and microvessel hematocrit in the mesentery of the cat, Microvasc Res 19(3), 297-319 (1980).
9. B. R. Duling and R. M. Berne, Longitudinal gradients in periarteriolar oxygen tension: A possible mechanism for participation of oxygen in local regulation of blood flow, Circ Res 27(5), 669-678 (1970).
10. J. B. Bassingthwaighte, I. S. J. Chan and C. Y. Wang, Computationally efficient algorithms for convection-permeation-diffusion models for blood-tissue exchange, Ann Biomed Eng 20(6), 687-725 (1992).
11. K. Dalziel and J. R. P. O'Brien, The kinetics of deoxygenation of human haemoglobin, Biochem J 78(236-245 (1961).
12. J. M. Vanderkooi, G. Maniara, T. J. Green and D. F. Wilson, An optical method for measurement of dioxygen concentration based upon quenching of phosphorescence, J Biol Chem 262(12), 5476-5482 (1987).